Medicon Engineering Themes
Volume 3 Issue 3 September 2022
Research Article

Experimental Study on Moisture Loss Mechanism in Apples Tissue

Georges El Achkar[1,2]* Bin Liu[1] and Rachid Bennacer[3]

[1]*Tianjin University of Commerce, Guangrong Rd 409, Tianjin, 300134, China*

[2]*Defence and Security Research Institute, University of Nicosia, Nicosia, CY 2417, Cyprus*

[3]*Paris-Saclay University, 61 Avenue du Président Wilson, 94235 Cachan, France*

***Corresponding Author:** Georges El Achkara, Tianjin University of Commerce, Guangrong Rd 409, Tianjin, 300134, China; Defence and Security Research Institute, University of Nicosia, Nicosia, CY 2417, Cyprus.

Received: August 11, 2022; **Published:** August 30, 2022

DOI: 10.55162/MCET.03.075

Abstract

In this paper, the moisture loss mechanism in biological tissue of apples was experimentally investigated in order to understand this mechanism and hence to extend their shelf life. An image conversion procedure, based on the use of image processing and AlgoLab Photo Vector softwares, was developed in order to characterise physically the internal porous structure of apples from the core to the skin. Several geometrical and physical parameters of the restructured porous media (porosity, fractal dimension, tortuosity, capillary pressure, permeability) were determined, and a comparison between their trends was carried out and analysed. Besides, a moisture loss model was established and discussed.

Keywords: bioproduct; apple; biological tissue; porous media; dehydration; experimentation

Nomenclature

A: pores area (m^2).
A_0: cross-section area of porous media (m^2).
d: diameter (m).
D: dimension (-).
f: probability density function (-).
F: shape factor (-).
L: length (m).
L_0: length along the pressure gradient direction (m).
P: pressure (Pa).
Q: volumetric flow rate ($m^3.s^{-1}$).
R: radius (m).
S: area (m^2).
u: superficial velocity ($m.s^{-1}$).

Greek symbols

Δ: difference (-).
K: permeability (-).
μ: dynamic viscosity (Pa.s)
ϕ: porosity (-).
σ: surface tension (N.m).
τ: tortuosity (-).
θ: contact angle (∘).

Subscripts

c: capillary.
f: fractal
g: gravitionalm mechanical max maximum min minimum.
R: radial.
T: tortuosity.
V: vacuum.

Introduction

The water content in bioproducts (fruits and vegetables) is the key factor affecting their quality during the storage process. Despite the numerous studies available in the literature, the evolutions during storage time of the thermophysical properties and the water transfer within bioproducts are still not well understood yet. Indeed, several heat and mass transfer aspects within bioproducts were highlighted, as during vacuum cooling for cylindrical vegetables (Chen et al., 2011) and spherical fruits (Su and He, 2009; Li, 2011) and during drying process for litchi (Janjai et al., 2010) and apple (Askari et al., 2013). The weight of the osmotic dehydration at a storage temperature above 0°C was undertaken by Kaminska et al. (2008) for apple and by Ruiz-Lopez et al. (2011) for other spherical fruits. However, these studies did not take into account the inner complex structure of the biological tissue and used limited homogeneous approach. Thereby, the geometrical and physical characterisation of the biological tissue and the study of the water transfer mechanism are of great interest.

In this study, we focused on the identification of the inner biological structure of a bioproduct in order to understand the water transfer mechanism. The geometrical characteristics of this porous media were determined and analysed, and the significant effects of some parameters on the water transfer mechanism were highlighted.

Materials and experimental protocol

The bioproducts chosen were 5 Fuji apples selected at a same maturity and a uniform size with no disease and damage. The experiments were carried out in a relatively short duration and so the effect of time on the moisture loss mechanism of apple was not studied. The equipment used to reach the scientific goal is: a cooling chamber for temperature and relative humidity control, a slicing machine (VT1000S/Leica) for samples preparation and a microscope (BX51/Olympus) for tissue observation. In order to get a realistic apple's internal structure, the fractal porous media structuration was followed. The obtained microscopic images of the apples slices were converted into geometrical structures. The Fig. 1 shows the conversion procedure of the microscopic image consisted of the following four steps:

1. Acquisition of the non-deformed apple's structure image using the microscope (Fig. 1a);
2. Scan of the rough microscopic image, reduction of its noise and adjustment of the grey threshold (Richmond, 2009) using Adobe Photoshop software (Fig. 1b);

3. Binarisation of the processed image using Matlab software (Fig. 1c);
4. Conversion of the binary image to a geometrical figure using AlgoLab Photo Vector software (Fig. 1d).

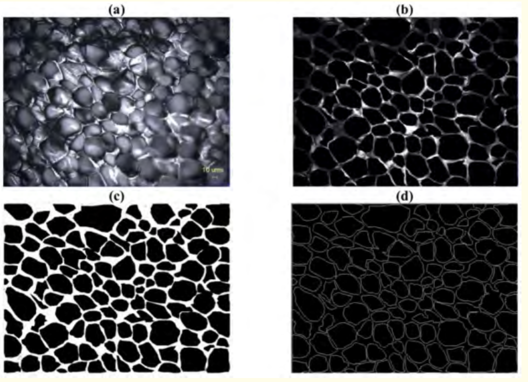

Figure 1: Conversion procedure of the microscopic image; (a) rough image; (b) processed image; (c) binarised image; (d) converted image.

In order to get a deep understanding of the apple's internal structure, and assuming that the apple is perfectly spherical with a radius R, slices were taken at different radial positions of 0.25R, 0.5R, 0.75R, 0.95R and 1R (skin), respectively, as shown in Fig. 2.

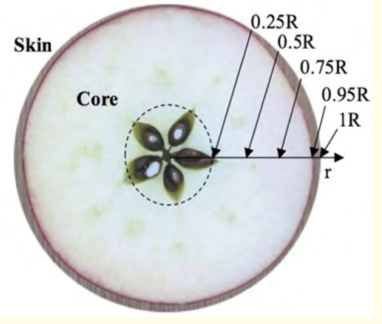

Figure 2: Simplified representative schematic of apple.

Using the previously described procedure, the rough, binarised and converted microscopic images of the considered apple's slices are represented in Fig. 3. As it can be noticed, the cells distribution is denser near the core and at the skin than at the other radial positions.

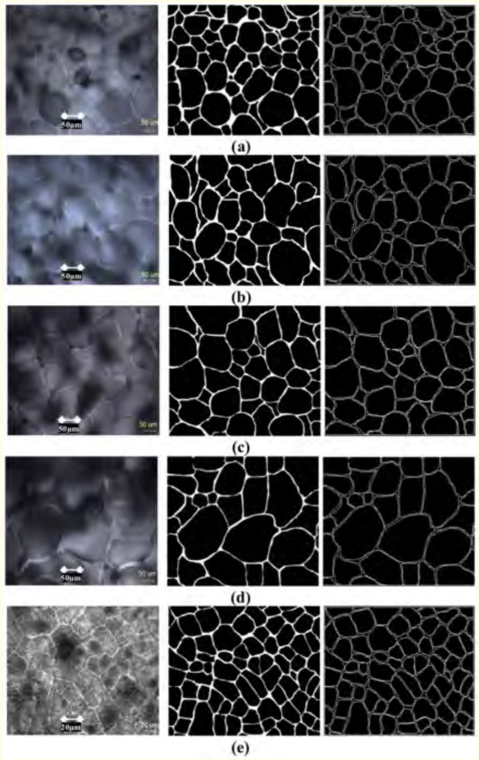

Figure 3: Rough (left), binarised (middle) and converted (right) microscopic images of apple's slices at different radial positions of (a) 0.25R, (b) 0.5R, (c) 0.75R, (d) 0.95R and (e) 1R.

Geometrical characterisation

For such two-dimensional structure we can define the porosity, the elementary structure (shape and size) and eventually the tortuosity, which could be deduced from the two previous properties. The porosity is the ratio of the pores volume to the total volume of the porous media, which can also refer to the fraction of void space in the porous media. In two-dimensional case, the porosity (ϕ) is defined as follows:

$$\phi = \frac{A}{A_0} \qquad (1)$$

Where A and A_0 are the pores area and the total cross-section area of the porous media, respectively. The binarised microscopic image consists of a binary matrix whose elements are of values 1 and 0, where the value 1 (white) represents the pores and the value 0 (black) represents the solid. Hence, the ratio of the points of value 1 to the total points gives the porosity. The regular cells geometry could be identified by a medium size defined as a fractal dimension. The computing method of this fractal dimension is based on the Minkowski Bouligand dimension, consisting in laying the fractal on an evenly spaced grid and counting how many boxes are required to cover the set. The box-counting dimension is calculated by seeing how this number changes as we make the grid finer by applying a box-counting algorithm. Assuming that N(ϵ) is the number of boxes of side length ϵ required to cover the set, then the fractal dimension (D_f) is defined as (Zhu and Ji, 2011):

$$D_f = \lim_{\epsilon \to 0} \frac{\log_{10}[N(\epsilon)]}{\log_{10}[1/\epsilon]} \qquad (2)$$

The evolution of $\log_{10}[N(\epsilon)]$ as a function of $-\log_{10}[\epsilon]$ was obtained thanks to Matlab software and reported in Fig. 4. The obtention of a linear curve means that a characteristic length exists. The slope of this curve corresponds thus to the fractal dimension (Ning and Zhang, 2013).

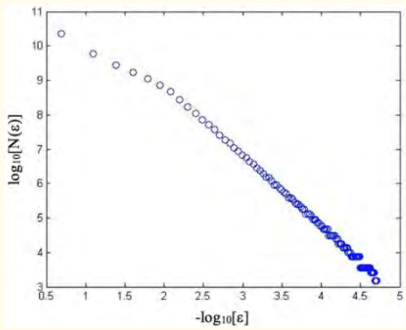

Figure 4: Evolution of $\log_{10}[N(\epsilon)]$ as a function of $-\log_{10}[\epsilon]$.

Yu and Li (2004) defined the tortuosity (τ) for flow through a two-dimensional porous media as:

$$\tau = \frac{1}{2}\left[1 + \frac{1}{2\sqrt{1-\phi}} + \sqrt{1-\phi}\frac{\sqrt{\left(\frac{1}{\sqrt{1-\phi}}-1\right)^2 + \frac{1}{4}}}{1-\sqrt{1-\phi}}\right] \qquad (3)$$

The identified geometrical properties could be related to the capillary pressure (caused by surface tension) and the permeability, which control the apple's dehydration.

Results and discussion

The physical phenomena controlling the mass transfer in a porous structure are the pores area, the curvature affecting the pressure difference and the water content (i.e. concentration) inducing the osmotic potential. The analysis of the 5 apples slices at the different radial positions from the core to the skin allows getting the porosity, the fractal dimension and the tortuosity. The corresponding results are summarised in Tables 1, 2 and 3.

Radial position ***Sample***	***0.25R***	***0.5R***	***0.75R***	***0.95R***	***1R***
1	0.1391	0.122	0.0915	0.0861	0.1364
2	0.1208	0.1125	0.1206	0.0929	0.1554
3	0.1287	0.0921	0.1137	0.0902	0.1217
4	0.1518	0.103	0.0948	0.0944	0.2002
5	0.1132	0.0937	0.0922	0.1249	0.1482
Average of samples	0.13072	0.10466	0.10256	0.0977	0.15238

Table 1: Porosity of apples slices.

Radial position / Sample	0.25R	0.5R	0.75R	0.95R	1R
1	1.6870	1.6359	1.6028	1.5463	1.7114
2	1.6567	1.6204	1.6463	1.5578	1.7342
3	1.6565	1.5736	1.6566	1.5633	1.6166
4	1.6848	1.6328	1.6322	1.5717	1.778
5	1.6636	1.5945	1.6144	1.6893	1.7293
Average of samples	1.66972	1.61144	1.63046	1.58568	1.7139

Table 2: Fractal dimension of apples slices.

Radial position / Sample	0.25R	0.5R	0.75R	0.95R	1R
1	4.0229	4.5196	5.8733	6.2139	4.0929
2	4.5598	4.8617	4.5666	5.7915	3.6530
3	4.309	5.8379	4.8153	5.9515	4.5295
4	3.7277	5.2678	5.6844	5.7066	2.9534
5	4.8345	5.7459	5.8321	4.4256	3.8062
Average of samples	4.29078	5.24658	5.35434	5.61782	3.807

Table 3: Tortuosity of apples slices.

The Fig. 5 shows the evolution of the apples porosity as a function of their radial position. The porosity decreases weakly then increases, reaching its maximum value at the skin. The porosity reaches the minimum value at the radial position of 0.95R (i.e. just under the skin). This result is coherent with the images of Fig. 3, which show that the skin cells size is the smallest and the arrangement is the closest at this position.

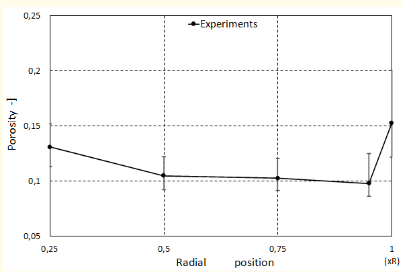

Figure 5: Evolution of the apples porosity as a function of their radial position.

The Fig. 6 shows the evolution of the apples fractal dimension as a function of their radial position. The fractal dimension has the same trend as the porosity, namely that it increases with the porosity increase and decreases with the porosity decrease. These two tendencies illustrate the global homothety where the flux cross surface increases with the porosity increase and the induced pressure difference related to curvature is expressed as a fractal dimension dependency. The Fig. 7 shows the evolution of the apples tortuosity as a function of their radial position. The tortuosity has the inverse trend of the porosity, namely that it increases with the porosity decrease and decreases with the porosity increase. The structure changes affect the tortuosity specific area, inducing an evolutive apparent permeability.

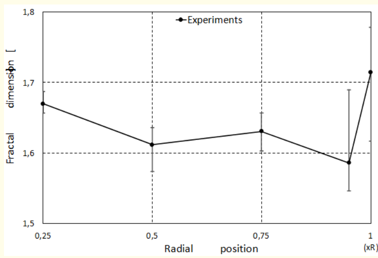

Figure 6: Evolution of the apples fractal dimension as a function of their radial position.

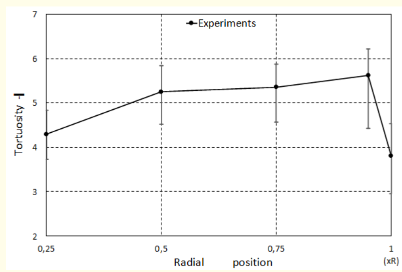

Figure 7: Evolution of the apples tortuosity as a function of their radial position.

Usually, the pressure in such a complex evolutive structure refers to the applied mechanical pressure. However, in a general sense, the pressure should also include gravitational, vacuum, and capillary pressures. As we have no access to constitute the evolution of the considered biological structured cells, we assume that it remains constant (i.e. no significant relative change). Thus, the pressure difference (ΔP) can be expressed as (Ahn et al., 1911):

$$\Delta P = P_m + P_g + P_v + P_c \qquad (4)$$

Where P_m, P_g, P_v and P_c are the mechanical, gravitational, vacuum and capillary pressures, respectively. This pressure controls the water transfer and hence the apple's dehydration. In the present study, we mainly focused on the capillary pressure and the contribution on the dynamic pressure. In a single capillary, Ahn et al. (1911) established the capillary pressure equation as follows:

$$P_c = \frac{F}{d_c}\left(\frac{1}{\phi} - 1\right)\sigma cos(\theta) \qquad (5)$$

Where F is the shape factor depending on the geometry and the fluid flow direction, d_c is the capillary (i.e. pore) diameter, σ is the surface tension of the liquid phase and θ is the contact angle between the liquid and solid phases. The average capillary pressure of the porous media is hence determined by:

$$\bar{P}_c = \int_{d_{c,min}}^{d_{c,max}} P_c f(d_c) \partial d_c \qquad (6)$$

With

$$f(d_c) = D_f d_{c,min}^{D_f} d_c^{-(D_f+1)} \quad (7)$$

Where f(dc) is the probability density function of the pores distribution and $d_{c,min}$ and $d_{c,max}$ are the minimum and maximum capillary diameters, respectively. By inserting the Eq. 7 in the Eq. 6, the average capillary pressure becomes:

$$\bar{P}_c = F\sigma cos(\theta)\frac{D_f}{\phi}\left(\frac{1-\phi}{D_f+1}\right)\left[\frac{1}{d_{c,min}} - \frac{1}{d_{c,max}}\left(\frac{d_{c,min}}{d_{c,max}}\right)^{D_f}\right] \quad (8)$$

According to Yu and Cheng (2002):

$$\left(\frac{d_{c,min}}{d_{c,max}}\right)^{D_f} = 0 \quad (9)$$

Hence:

$$\bar{P}_c = \frac{F}{d_{c,min}}\sigma cos(\theta)\frac{D_f}{\phi}\left(\frac{1-\phi}{D_f+1}\right) \quad (10)$$

From the Eq. 10, we can notice that the average capillary pressure in porous media is related to the shape factor, the minimum capillary diameter, the surface tension, the contact angle, the porosity and the fractal dimension. The value of the average capillary pressure is generally ranging between 10^3 and 10^4 Pa (Yu and Cheng, 2002). In our study, this average capillary pressure wad calculated by considering the different parameters as follows:

- Shape factor: $F = \frac{4S}{L^2}$ (Amico and Lekakou, 2001);
- Minimum capillary diameter: $d_{c,min}$ measured directly using Image-Pro Plus software;
- Surface tension: $\sigma = 0.044$ N.m^{-1};
- Contact angle: $\theta = 57 \circ$ (Yu and Cheng, 2002);
- Porosity: ϕ as defined in Eq. 1;
- Fractal dimension: D_f as defined in Eq. 2.

Due to the capillary pressure effect, the fractal permeability model of the porous media is deduced as follows (Liu et al., 2007):

$$\kappa = \frac{\pi L_0^{1-D_T} D_f F\sigma cos(\theta)\left(\frac{1-\phi}{\phi}\right) d_{c,max}^{2+D_T}}{128A\Delta P(2+D_T-D_f)}\left[1-\left(\frac{d_{c,min}}{d_{c,max}}\right)^{2+D_T-D_f}\right] \quad (11)$$

Where L_0 is the length of a straight distance along the microscopic pressure gradient direction and D_T is the tortuous dimension. This fractal permeability model can be calculated as follows:

- $d_{c,min}$ and $d_{c,max}$ are directly measured using Image-Pro Plus software;
- $L_0 = A^{0.5}$ and $D_T = 1.1$ (Fu and Shen, 2007).

For apple sample 1, the capillary pressure, permeability, and minimum and maximum capillary diameters at the radial positions 0.25R, 0.5R, 0.75R, 0.95R and 1R (skin) were calculated, and the results are reported in Table 4. As it can be noticed, the capillary pressure and the permeability have the same developing trend, both of them increase as the radius increases. They reach the maximum value at the position of 0.95R, and then begin to decrease. The permeability and the capillary pressure are inversely proportional to porosity. The smaller porosity is, more remarkable the changes of the capillary pressure and the permeability are, as shown in Figs. 8, 9 and 10.

Radial position [m]	*Porosity [-]*	*Fractal dimension[-]*	*Minimum capillary diameter [m]*	*Maximum capillary diameter [m]*	*Capillary pressure [Pa]*	*Permeability [m²]*
0.25R	0.139	1.687	1.38×10^{-6}	2.6×10^{-5}	141.98	1.73×10^{-14}
0.5R	0.122	1.636	1.09×10^{-6}	9.93×10^{-6}	240.096	7.32×10^{-16}
0.75R	0.092	1.603	6.9×10^{-7}	1.27×10^{-5}	392.42	1.33×10^{-15}
0.95R	0.086	1.546	5.56×10^{-7}	1.3×10^{-5}	678.43	3.86×10^{-15}
1R	0.136	1.711	4.36×10^{-7}	7.17×10^{-6}	345.42	7.18×10^{-16}

Table 4: Capillary pressure, permeability, and minimum and maximum capillary diameters for apple sample 1.

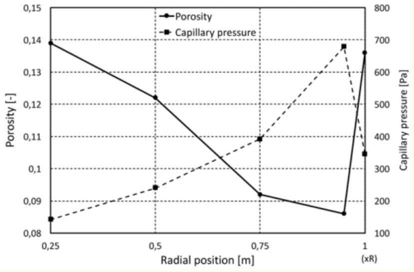

Figure 8: Evolutions of the apples porosity and capillary pressure as a function of their radial position.

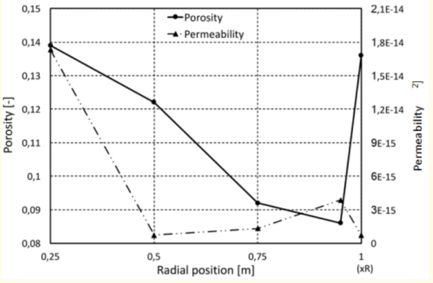

Figure 9: Evolutions of the apples porosity and permeability as a function of their radial position.

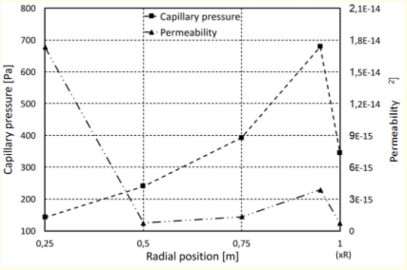

Figure 10: Evolutions of the apples capillary pressure and permeability as a function of their radial position.

Model of moisture loss

As a porous media, the apple's internal moisture transfer process is described by Darcy's law as follows:

$$u_R = \frac{Q_R}{A} = -\frac{\kappa}{\mu}\frac{dP_c}{dR} \qquad (12)$$

Where u_R and Q_R are the superficial velocity and the volumetric flow rate in the radial direction, respectively, A is the cross-sectional area normal to the flow direction and μ is the dynamic viscosity. According to this law, we can notice that the main factors influencing the moisture transfer in the porous media are the capillary pressure and the permeability. The Eqs. 10 and 11 indicate that the main factors affecting these capillary pressure and permeability are the minimum and maximum capillary diameters, the porosity, the fractal dimension, etc. However, the minimum capillary diameter has the greatest impact on the capillary pressure, as shown in Fig. 11, and the maximum capillary diameter and the porosity have the greatest impact on the permeability, as shown in Fig. 12.

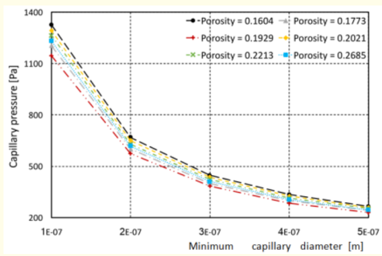

Figure 11: Evolution of the apples capillary pressure as a function of their minimum capillary diameter for different porosities.

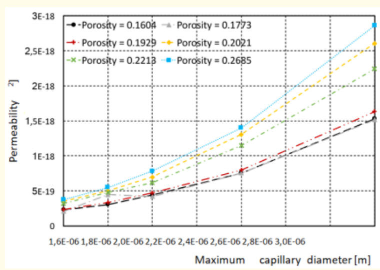

Figure 12: Evolution of the apples permeability as a function of their maximum capillary diameter for different porosities.

Since the porosity is the ratio of the pores area to the total area, for the same porosity, the porous media can have different structures and hence different minimum and maximum capillary diameters. In summary, the minimum and maximum capillary diameters are the most important parameters affecting the moisture transfer in a porous media. This aspect is due to the complexity and irregularity of the actual porous media. For the porous media having the same porosity and fractal dimension, the capillary pressure increases with the increase of the minimum capillary diameter and the permeability increases with the increase of the maximum capillary diameter.

Conclusions and perspectives

An experimental study on the moisture loss mechanism in biological tissue of apple was conducted. An image conversion procedure, based on the use of image processing and AlgoLab Photo Vector softwares, was developed in order to characterise physically the internal porous structure of apple from the core to the skin. The porosity, the fractal dimension, the tortuosity, the capillary pressure and the permeability of the restructured porous media were determined, and the following main conclusions were highlighted:

- The apple is a porous media with a fractal characteristic.
- As the apple's radial position increases, the porosity first decreases and then increases. The minimum porosity is just under the skin and the maximum porosity is at the skin.
- The fractal dimension has the same trend as the porosity, namely that it increases with the porosity increase and decreases with the porosity decrease.
- The permeability and the capillary pressure are inversely proportional to the porosity, namely that they increase with the porosity decrease and decrease with the porosity increase.
- The main factors influencing the moisture transfer in a porous media are the porosity, the capillary pressure and the permeability.
- The impact on moisture transfer in a porous media is inversely proportional to the porosity.
- The capillary pressure in a porous media is inversely proportional to the minimum capillary diameter.
- The permeability in a porous media is proportional to the maximum cap-illary diameter.

A complementary study concerning the moisture loss in biological tissue of apple during hyo-on storage is in progress, in order to study the effect of time on the apple dehydration for various storage conditions. Additional studies on other bioproducts are of great interest, in order to find a generalised correlation for bioproducts dehydration.

Acknowledgements

Financial support from the National Natural Science Foundation of China is gratefully acknowledged.

References

1. Ahn KJ, Seferis JC and Berg JC. "Simultaneous measurements of permeability and capillary pressure of thermosetting matrices in woven fabric reinforcements". Polymer Composites 12.3 (1911): 146-152.
2. Amico S and Lekakou C. "An experimental study of the permeability and capillary pressure in resin-transfer moulding". Composites Science and Technology 61 (2001): 1945-1959.
3. Askari GR, Emam-Djomeh Z and Mousavi SM. "Heat and mass transfer in apple cubes in a microwave-assisted fluidized bed drier". Food and Bioproducts Processing 91.3 (2013): 207-215.
4. Chen X, Han H and Kan A. "Study on mass and heat loss of porous vegetables during vacuum cooling". Anhui Agricultural Science Bulletin 17.5 (2011): 143-145.
5. Fu R and Shen H. "Automatically discriminating overlapped cell based on shape factor analysis: a technical study". Military Medical Sciences 31.5 (2007): 463465.
6. Janjai S., et al. "Diffusivity, shrinkage and simulated drying of litchi fruit (litchi chinensis sonn.)". Journal of Food Engineering 96.2 (2010): 214-221.
7. Kaminska A, Lewicki PP and Malczyk P. "Mass transfer in osmotically dehydrated apple stored at temperatures above zero". Journal of Food Engineering 86 (2008): 140-149.
8. Li W. "The numerical simulation analytical study on the drying process of dates". Master thesis, Jilin University (2011).
9. Liu Y., et al. "Study of the effect of capillary pressure on permeability". Fractals 15.1 (2007): 55-62.
10. Ning J and Zhang W. "Microcosmic fractal image processing based on matlab". Computer and Modernization 1.2 (2013): 5-8+14.

11. Richmond J. “Steady state thermal conductivity”. Master thesis, Tianjin University (2009).
12. Ruiz-Lopez et al. “Modeling and simulation of heat and mass transfer during drying of solids with hemispherical shell geometry”. Computers and Chemical Engineering 35 (2011): 191199.
13. Su Q and He G. “Heat/mass transfer analysis and numerical simulation for vacuum storage of pear”. Vacuum 46.1 (2009): 73-77.
14. Yu B and Cheng P. “A fractal permeability model for bi-dispersed porous media”. International Journal of Heat and Mass Transfer 45 (2002): 2983-2993.
15. Yu B and Li J. “A geometry model for tortuosity of flow path in porous media”. Chinese Physics Letters 21 (2004): 1569-1571.
16. Zhu H and Ji C. “Fractal theory and its applications”. Beijing Science Press (2011).

Volume 3 Issue 3 September 2022